Ceramics International **21** (1995) 339–343

Zirconia–Alumina Particulate Composites by Infiltration Processing

S. Riou, F. Queyroux & Ph. Boch

Ecole Supérieure de Physique et de Chimie Industrielles, 10, rue Vauquelin – 75231 Paris Cedex 05, France

(Received 27 October 1994; accepted 8 February 1995)

Abstract: ZrO_2–Al_2O_3 particulate composites were prepared by infiltration of pre-sintered alumina skeletons with a precursor of zirconia and subsequent sintering at 1600°C. The composite specimens exhibit a gradient in composition, the zirconia content being higher in the superficial zones than in the core. The influence of the ZrO_2 content on the volume fraction of t-ZrO_2, the t→m transformation temperature, and the microstructural development were studied.

1 INTRODUCTION

The paper examines the potential of infiltration processing for controlling the distribution and the microstructural development of an unstabilized zirconia phase in an alumina matrix. The infiltration process, similar to that initiated by Marple and Green,[1] was used to incorporate zirconia into pre-sintered, porous alumina bodies. Infiltration allows the preparation of ceramic composites with gradients in composition and microstructure.[2,3]

2 EXPERIMENTAL

2.1 Pre-sintering, infiltration and sintering

The alumina powder was a P172-SB Aluminium-Péchiney grade, with a composition of 99·70 Al_2O_3, 0·05 Na_2O, 0·05 CaO, 0·08 SiO_2, 0·02 Fe_2O_3, and 0·10 MgO (in wt%). The mean particule size was 0·75 μm. Polyvinylbutyral (2·5 wt%) was added to the powder as a binder.

After granulation, the powder was uniaxially pressed under 150 MPa. The powder compacts were cylindrical pellets (13 mm in diameter and 4 mm in height) or prismatic bars (35 mm × 7 mm × 4·5 mm).

The compacts were pre-sintered at 1000°C (heating rate of 10°C min^{-1}, soaking time of 3 h) and then cooled (at 10°C min^{-1}) to room temperature. The relative density of pre-sintered samples was about 62%. A mercury intrusion technique showed that the pore size distribution was homogeneous, with nearly-monosized pores of 100 nm in mean diameter. Various tests indicated that a pre-sintering temperature of 1000°C was the best compromise between lower temperatures, leading to a higher porosity but a higher brittleness, and higher temperatures, leading to a better toughness but a lower porosity.

The infiltrated liquid was an aqueous solution of zirconyl chloride octahydrate ($ZrOCl_2$, $8H_2O$). This solution readily infiltrates the pre-sintered alumina and it decomposes at 900°C, which is well below the sintering temperature of 1600°C. Two concentrations were used:

(i) A concentrated solution with a density of 1·48 g cm^{-3} and a conversion yield into zirconia of 23·7 wt%.
(ii) A diluted solution with a density of 1·22 g cm^{-3} and a conversion yield into zirconia of 14·0 wt%.

The porous preforms were de-aerated under primary vacuum for 45 min, then infiltrated by immersing them in the solution for a time of 30 min. This time was necessary to be sure that the infiltration front had reached the center of the

Ceramics International Printed in Great Britain

preform. The filling of pores by the solution was close to 98%. The infiltrated preforms were dried at 100°C for 24 h, by holding them so that all their faces were equally exposed to the surrounding atmosphere, to limit the liquid segregation.[2] Then, they were heated to 900°C (heating rate of 10°C min^{-1}, soaking time of 2 h) to decompose the infiltrant, cooled to room temperature, and infiltrated again. Multiple infiltrations allowed us to increase the zirconia content in the composites.

Finally, the infiltrated samples were sintered at 1600°C (heating rate of 10°C min^{-1}, soaking time of 2 h, cooling rate of 20°C min^{-1}), using an electric furnace with $MoSi_2$ heating elements.

2.2 Characterization

The zirconia content in the sintered bodies was determined by measuring the weight difference before infiltration and after sintering. Several series of samples were prepared and labelled as A_{ij}, B_{ij}, C_{ij}, etc., $<<i>>$ being the number of infiltrations with the concentrated solution and $<<j>>$ the number of infiltrations with the diluted solution.

XRD was performed on the faces of the cylindrical pellets, using Cu-$K_{\alpha 1}$ radiation. A dilatometric study was made between room temperature and 1400°C (heating and cooling rates of 3°C min^{-1}). Microstructural investigations were carried out on one of the two faces of the cylindrical samples by SEM. The surface was polished with diamond pastes and thermally etched at 1500°C for 24 min to reveal the microstructure.

3 RESULTS AND DISCUSSION

3.1 X-ray diffraction

XRD was used to study the gradient of zirconia content within the samples, its dependence vs the infiltration procedure, and to determine the ratio of t-ZrO_2 to m-ZrO_2.

Standards of known compositions were prepared by mixing α–Al_2O_3 and m-ZrO_2 powders. Three XRD peaks were considered, namely α-Al_2O_3 (102), m-ZrO_2 (111), and m-ZrO_2 ($11\bar{1}$). The peaks are located in the range of $24° < 2\theta < 32°$. With:

$$X = wt_{ZrO_2}/wt_{Al_2O_3}$$

and

$$Y = [I_m(111)+I_m(11\bar{1})]/I_{Al_2O_3}(102)$$

it was found that the weight ratio (X) and the peak height ratio (Y) were linked by the experimental law: $X = 0{\cdot}09\ Y$.

Toraya *et al.*[4] have established that the ratio (P) defined by

$$P = \frac{I_t(111)}{I_m(111)+I_m(11\bar{1})}$$

is equal to 1·34 for zirconia. In this expression, the tetragonal structure is described by a tetragonal cell with $a = 0{\cdot}514$ nm and $c = 0{\cdot}527$ nm.

Taking into account that both monoclinic and tetragonal zirconia are present, we have considered parameter P^*, which is related to P by the following expression

$$P^* = P[d_{m\text{-}ZrO_2}/d_{t\text{-}ZrO_2}] \approx 0{\cdot}95\ P$$

with $d_{m\text{-}ZrO_2} = 5{\cdot}83$ g cm^{-3} and $d_{t\text{-}ZrO_2} = 6{\cdot}10$ g cm^{-3}. Consequently, the peak height ratio (Y) and the relative volume fraction of t-ZrO_2 when both t-ZrO_2 and m-ZrO_2 were present in a given sample are:

$$Y = I_t(111)+P^*[I_m(111)+I_m(11\bar{1})]/P^*\ I_{Al_2O_3}(102)$$

$$t\text{-}ZrO_2(vol\%) = I_t(111) \times 100/I_t(111)+P[I_m(111)+I_m(11\bar{1})]$$

Data were collected using six series of samples: A01, A10, A11, A20, A30, and A40. For a given sample, the average zirconia content (C) was determined using the weight difference between non-infiltrated samples and sintered infiltrated samples:

$$C\ (wt\%) = wt_{ZrO_2} \times 100/[wt_{Al_2O_3}]$$

The content of ZrO_2 in the superficial zone (C_s) was deduced from XRD data. Table 1 shows the results, for various infiltration procedures.

Table 1. Effect of the infiltration procedure on C, C_s and the fraction of t-ZrO_2

Sample	Average ZrO_2 content (C, in wt%)	Superficial ZrO_2 content (C_s, in wt%)	C_s/C	Relative volumic fraction of t-ZrO_2 in the superficial region (%)
A01	2·3	14·5	6·3	95
A10	5·2	12·3	2·4	91
A11	7·6	20·0	2·6	48
A20	10·2	20·6	2·0	44
A30	13·8	24·8	1·8	11
A40	17·4	30·0	1·7	4

Table 2. Relative volumic fractions of ZrO_2 for the two limit cases where zirconia is entirely tetragonal (V_t) or entirely monoclinic (V_m)

Sample	V_t (vol%)	V_m (vol%)
A01	1·5	1·6
A10	3·4	3·6
A11	5·1	5·3
A20	6·9	7·2
A30	9·4	9·8
A40	12·0	12·5

It can be seen that C_s is always higher than C, which is in agreement with the results of Marple and Green.[2,3] However, the C_s/C ratio decreases when the infiltration number increases (compare A10, A20, A30 and A40). This can be explained by a redistribution of the infiltrant liquid during the drying stage, such a redistribution being less easy when the pores become more filled. For a given number of infiltrations (compare A01 and A10), the C_s/C ratio is higher when the infiltration is carried out with the more diluted solution. The explanation is that the diluted solution is more fluid and, therefore, redistributes more easily. The relative fraction of t-ZrO_2 decreases when the infiltration number increases, which is due to the fact that the number of zirconia particles that exceed the critical size for the t→m transformation increases with the zirconia content.

The average volume fraction of zirconia within a sample cannot be estimated with high accuracy, because it depends on the t/m ratio, which can be measured on the *surface* only. However, this fraction (V) must be intermediate between V_t (that corresponds to 100% t-ZrO_2) and V_m (that corresponds to 100% m-ZrO_2). Table 2 shows that the difference between V_t and V_m is always small and that, therefore, $V \approx V_t \approx V_m$.

Multiple, successive abrasions were carried out on a low-zirconia (B10) and a high-zirconia (B40) pellet, to determine the ZrO_2-concentration profiles. However, abrasion damage can induce the t→m transformation of ZrO_2 particles. To eliminate the influence of this effect, a polishing treatment with fine diamond pastes was carried out after each abrasion, to eliminate the transformed layer. The thickness (e) of the removed zone was measured. Tables 3 and 4 give the concentration data and Fig. 1 shows the concentration profiles across the two samples.

Table 3. Relative volumic fraction and ZrO_2 content vs thickness (e) of the removed zone for sample B10. $C0$ = surface zirconia content before abrasion; $C(e)$ = surface zirconia content after abrasion and polishing

e (mm)	Relative volumic fraction of t-ZrO_2 (%)	$C(e)$ (wt% ZrO_2)	$C(e)/C0$
0·00	93	12·5	1·00
0·10	100	9·4	0·75
0·30	100	6·7	0·54
0·50	100	5·4	0·43
0·80	100	4·6	0·37
1·40	100	3·9	0·31
1·80	100	3·9	0·31

Table 4. Relative volumic fraction and ZrO_2 content vs thickness (e) of the removed zone for sample B40. $C0$ = surface zirconia content before abrasion; $C(e)$ = surface zirconia content after abrasion and polishing

e (mm)	Relative volumic fraction of t-ZrO_2 (%)	$C(e)$ (wt% ZrO_2)	$C(e)/C0$
0·0	3	31	1·00
0·20	4	26	0·84
0·40	7	24	0·77
0·55	10	22	0·71
0·70	13	19	0·61
0·80	17	19	0·61
1·00	21	17	0·55
1·20	30	17	0·55
1·40	34	16	0·52
1·60	37	14	0·45

All results confirm the three facts previously mentioned, namely: (i) a decrease in the ZrO_2 concentration with increasing distance from the surface, (ii) a decrease in the difference of ZrO_2 content between the surface and the core when the number of infiltration increases, and (iii) a decrease in the fraction of t-ZrO_2 when the ZrO_2 content increases.

3.2 Dilatometry

The study was made on five samples: C00, C10, C20, C30 and C40, corresponding to 0, 5·3, 9·7, 14·0 and 17·4 wt% of ZrO_2, respectively.

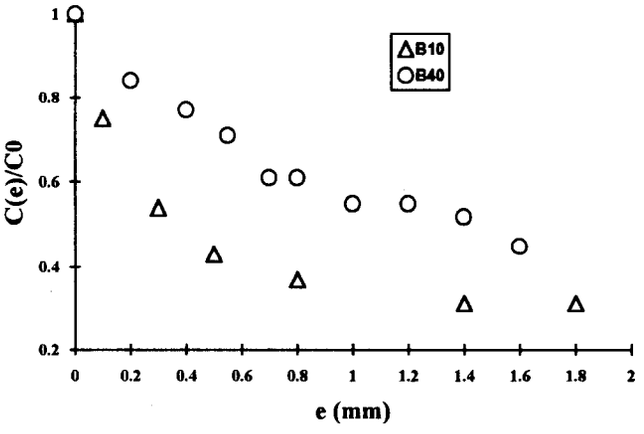

Fig. 1. Concentration profiles of zirconia in samples B10 (one infiltration) and B40 (four infiltrations).

Table 5. Influence of the ZrO_2 content on the t/m transformation temperature

Sample	Average ZrO_2 content (wt%)	α (10^{-6} K^{-1}) 400–1000°C	800–1300°C	Transformation temperature (°C) On heating	On cooling
C00	0	8·2	—	—	—
C10	5	9·6	—	—	—
C20	10	8·9	9·3	1080	650
C30	14	8·8	9·5	1090	725
C40	17	8·8	9·8	1090	760

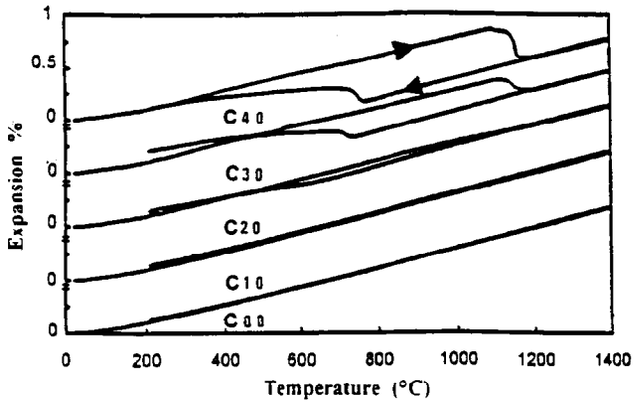

Fig. 2. Dilatometric curves.

As usual, the transformation of zirconia exhibits a hysteresic behavior. On heating, the m→t transition develops at about 1150°C. On cooling, the reverse transition develops at about 1030°C. This is accompanied by a volume increase of 5%.[5,6] Table 5 and Fig. 2 show the main data, α being the expansion coefficient.

The t→m transformation temperature decreases when the zirconia content decreases, which is associated with a decrease in the particle size and an increase in the mechanical constraint due to the matrix.[7,8] The area of the hysteresis cycle depends on the fraction of transformed zirconia.

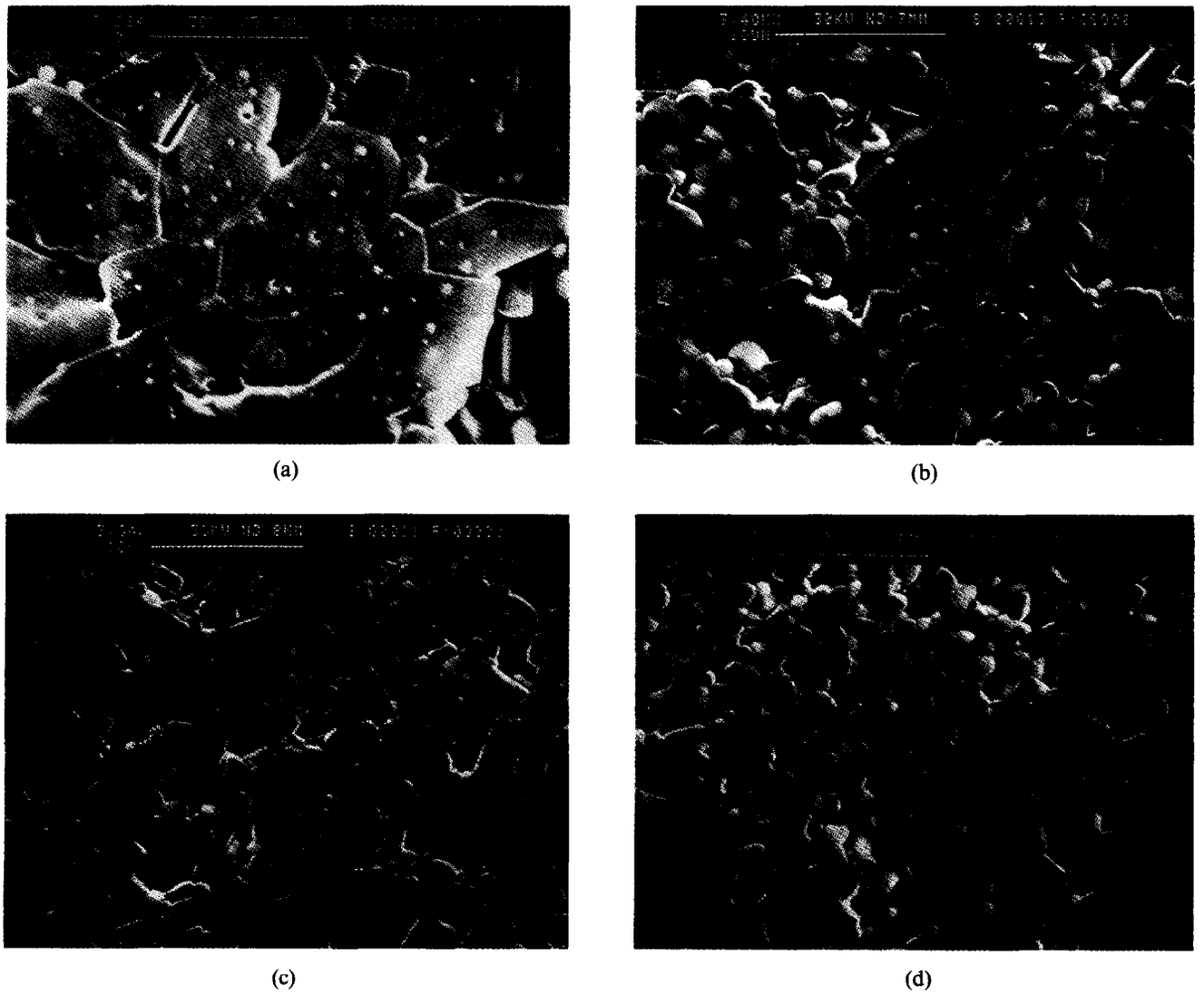

Fig. 3. SEM micrographs of materials sintered at 1600°C for 2 h. (a) A10, (b) A20, (c) A30 and (d) A40.

Table 6. Volumic fraction of zirconia in intragranular position and mean grain size of alumina

Sample	A10	A20	A30	A40
Fraction of intragranular ZrO_2 (vol%)	60	23	18	8
Mean grain size of Al_2O_3 (μm)	10	4	3	2

3.3 Microstructure

A microstructural study was made on samples A10, A20, A30 and A40 (Figs 3a–d). The grey zones are alumina, whereas the white zones are zirconia. The mean grain size of the alumina matrix was determined by a linear intercept method.[9]

In sintered samples, the mean grain size of the alumina matrix decreases when the zirconia content increases, which shows that ZrO_2 particles act as grain-growth inhibitors. Even for the lowest zirconia content, this grain size is smaller than that observed in ZrO_2-free alumina (14 μm).

In pre-sintered samples, the pores are mainly intergranular. After infiltration and heating, they are partially filled by zirconia. After sintering, the zirconia particles are predominantly intragranular in the samples with a low ZrO_2 content (Fig. 3a), whereas they are predominantly intergranular in the samples with a high ZrO_2 content (Figs 3b–d). For the highest zirconia contents (samples A30 and A40), ZrO_2 particles can move and merge to form larger aggregates and, therefore, ZrO_2/ZrO_2 grain boundaries can be observed.

4 CONCLUSION

The preparation of ZrO_2/Al_2O_3 particulate composites by infiltration of pre-sintered alumina preforms with zirconia precursor and subsequent sintering at 1600°C leads to composites with a gradient in composition. The zirconia content continually decreases from the surface to the core, but the composition difference decreases when the number of infiltrations increases. The gradient in composition induces a gradient in the microstructure.

ACKNOWLEDGMENT

The authors thank Mrs Chatry for her help in the SEM experiments.

REFERENCES

1. MARPLE, B. R. & GREEN, D. J., Mullite/alumina particulate composites by infiltration processing. *J. Amer. Ceram. Soc.*, **72**(11) (1989) 2043–48.
2. MARPLE, B. R. & GREEN, D. J., Mullite/alumina particulate composites by infiltration processing: II. Infiltration and characterization. *J. Amer. Ceram. Soc.*, **73**(12) (1990) 3611–16.
3. MARPLE, B. R. & GREEN, D. J., Graded compositions and microstructures by infiltration processing. *J. Mater. Sci.*, **28** (1993) 4637–43.
4. TORAYA, H., YOSHIMURA, M. & SOMIYA, S., Calibration curve for quantitative analysis of the monoclinic–tetragonal ZrO_2 system by X-ray diffraction. *J. Amer. Ceram. Soc.*, **67**(6) (1984) C119–21.
5. BANSAL, G. & HEUER, A. H., Martensitic transformation in zirconia. *Acta Metall.*, **20**(11) (1972) 1281–89.
6. PATIL, R. N. & SUBBARAO, E. C., Axial thermal expansion of ZrO_2 and HfO_2 in the range room temperature to 1400°C. *J. Appl. Cryst.*, **2** (1969) 281–88.
7. GARVIE, R. C. & GOSS, M. F., Intrinsic size dependence of the phase transformation temperature in zirconia microcrystals. *J. Mater. Sci.*, **21** (1986) 1253–57.
8. GARVIE, R. C., Thermodynamic analysis of the tetragonal to monoclinic transformation temperature in a constrained zirconia microcrystal. *J. Mater. Sci.*, **20** (1985) 3479–86.
9. WURST, J. C. & NELSON, J. A., Linear intercept technique for measuring grain size in two-phase polycrystalline ceramics. *J. Amer. Ceram. Soc.*, **55** (2) (1972) 109.